Quaternary Science Reviews 250 (2020) 106677

Contents lists available at ScienceDirect

Quaternary Science Reviews

journal homepage: www.elsevier.com/locate/quascirev

Multiple glacial maxima of similar extent at ~20–45 ka on Mt. Usborne, East Falkland, South Atlantic region

B.L. Hall [a, *], T.V. Lowell [b], P. Brickle [c]

[a] School of Earth and Climate Sciences and Climate Change Institute, University of Maine, Orono, ME, USA
[b] Department of Geology, University of Cincinnati, Cincinnati, OH, USA
[c] South Atlantic Environmental Research Institute, Stanley, Falkland Islands

ARTICLE INFO

Article history:
Received 16 April 2020
Received in revised form
11 September 2020
Accepted 25 October 2020
Available online xxx

Keywords:
South Atlantic
Falkland Islands
^{10}Be exposure age dating
Last glacial maximum

ABSTRACT

The pattern, timing, and origin of Southern Hemisphere climate change during the last glaciation remains a pressing problem, with implications for the role of orbital forcing in ice-age cycles. Here, we present geomorphological and cosmogenic exposure age data from East Falkland in the South Atlantic region that show onset of glacial conditions by marine isotope stage 4 (~60–70 ka), with expansion of ice to its maximum extent of the last glaciation. At least seven geomorphological units marked by multiple crests on composite moraines indicate glacier expansion on Mt. Usborne, the highest peak of East Falkland. From ~20 to 45 ka, glaciers fluctuated on a millennial timescale with near-maximum conditions being reached repeatedly. Overall ice extent appears to have shrunk slightly through time, with evidence of glaciation at ~20 ka preserved only in the highest-elevation cirques. This long glacial maximum is inconsistent both with local orbital control and orbital forcing as expressed in the traditional Milankovitch hypothesis. The timing of millennial glacier expansions occurred between Northern Hemisphere Heinrich Stadials and resembles that documented for New Zealand glaciers, suggesting at least a trans-Pacific expression. We postulate that periodic recessions corresponded with southward expansion of the southern westerlies during Heinrich Stadials and warming air and ocean temperatures over the South Atlantic region.

1. Introduction

The cause of ice-age cycles remains one of the most puzzling unsolved questions in earth sciences. The traditional view (Milankovitch, 1941) is that reduced summer insolation due to changes in orbital configuration caused cooling in high northern latitudes, leading to an ice age. However, this explanation does not adequately explain coeval Southern Hemisphere cooling, because, due to the effect of precession, insolation is out of phase with that in the north. This problem, highlighted by Mercer (1984) as the 'fly in the ointment of Milankovitch theory', has been addressed by suggesting that the northern signal can be propagated to the south through some as of yet uncertain mechanism (i.e., Broecker, 1998; Barker and Diz, 2014; Clark et al., 2009; Denton et al., 2010; Murray et al., 2012; Zhu et al., 2014). Others have suggested that southern insolation, driven primarily by obliquity, plays an important role in Southern Hemisphere climate (i.e., Fogwill et al., 2015). Still other work has led to the revival of the idea (Lorenz, 1968, 1975, 1976) that the earth's climate has at least two semi-stable states (glacial and interglacial) and can jump between them rapidly (a mode flip of Broecker and Denton, 1989) with little provocation or warning.

The last glacial maximum (LGM, "globally" 19–26.5 ka; Mix et al., 2001; Clark and Mix, 2002; Clark et al., 2009) in the Southern Hemisphere provides a test for assessing whether southern climate is driven predictably by northern insolation (through an intermediary, such as the bipolar seesaw or shifts in westerly winds), southern insolation, or neither. Recent analyses offer conflicting views into the workings of Southern Hemisphere climate during the LGM. For example, based on an analysis of South American cosmogenic exposure-age data, Fogwill et al. (2015) suggested that southern mid-latitude mountain glaciers reached their maximum extent at ~28 ka. They further hypothesized that this glacial maximum was linked to an obliquity minimum, which in their model caused colder temperatures in the southern mid-latitudes, vigorous atmospheric circulation, and an increase in Southern Ocean sea ice. Fogwill et al. (2015) also predicted gradual

* Corresponding author.
E-mail address: brendah@maine.edu (B.L. Hall).

https://doi.org/10.1016/j.quascirev.2020.106677
0277-3791/

glacier retreat after 28 ka, due to reduced precipitation caused by expansion of Southern Ocean sea ice. By this view, Southern Hemisphere climate is very closely coupled to southern, rather than northern insolation changes.

In contrast, a series of papers, based largely on cosmogenic isotope chronologies of New Zealand mountain glaciers (Putnam et al., 2013a,b; Kelley et al., 2014; Doughty et al., 2015; Shulmeister et al., 2018; Strand et al., 2019), but also in South America (i.e., Darvill et al., 2016) presents a view of long Southern Hemisphere glacial maximum, with repeated maxima from at least 42–18 ka (if not earlier, i.e., 65 ka of Schaefer et al., 2015), which apparently were unaffected by either the southern or northern insolation signals. Instead, millennial fluctuations superimposed on the long maximum were attributed to shifts in westerly winds, which affected local sea-surface temperatures and airflow on a Heinrich-stadial periodicity (Denton et al., 2010; Doughty et al., 2015), but the overall cause of such a long glacial maximum remains uncertain.

Detailed glacier records of the southern mid-latitude LGM at sites other than on the South American continent or in New Zealand are rare. Even in southern South America, many studies have focused on the termination or younger parts of the glacial maximum, with few (i.e., Garcia et al., 2018) adequately constraining older advances. Thus, to afford new evidence for the duration and structure of the LGM in the southern mid-latitudes, we examined the extent and timing of glaciation on the island of East Falkland in the South Atlantic region (Fig. 1).

Situated ~500 km off the southeastern coast of South America, the Falkland Islands lie in a climatically sensitive zone between the subantarctic and subtropical fronts. They also border the Southern Ocean, and cold water is transported adjacent to the island by the north-flowing Falkland Current. This current is a derivative of the

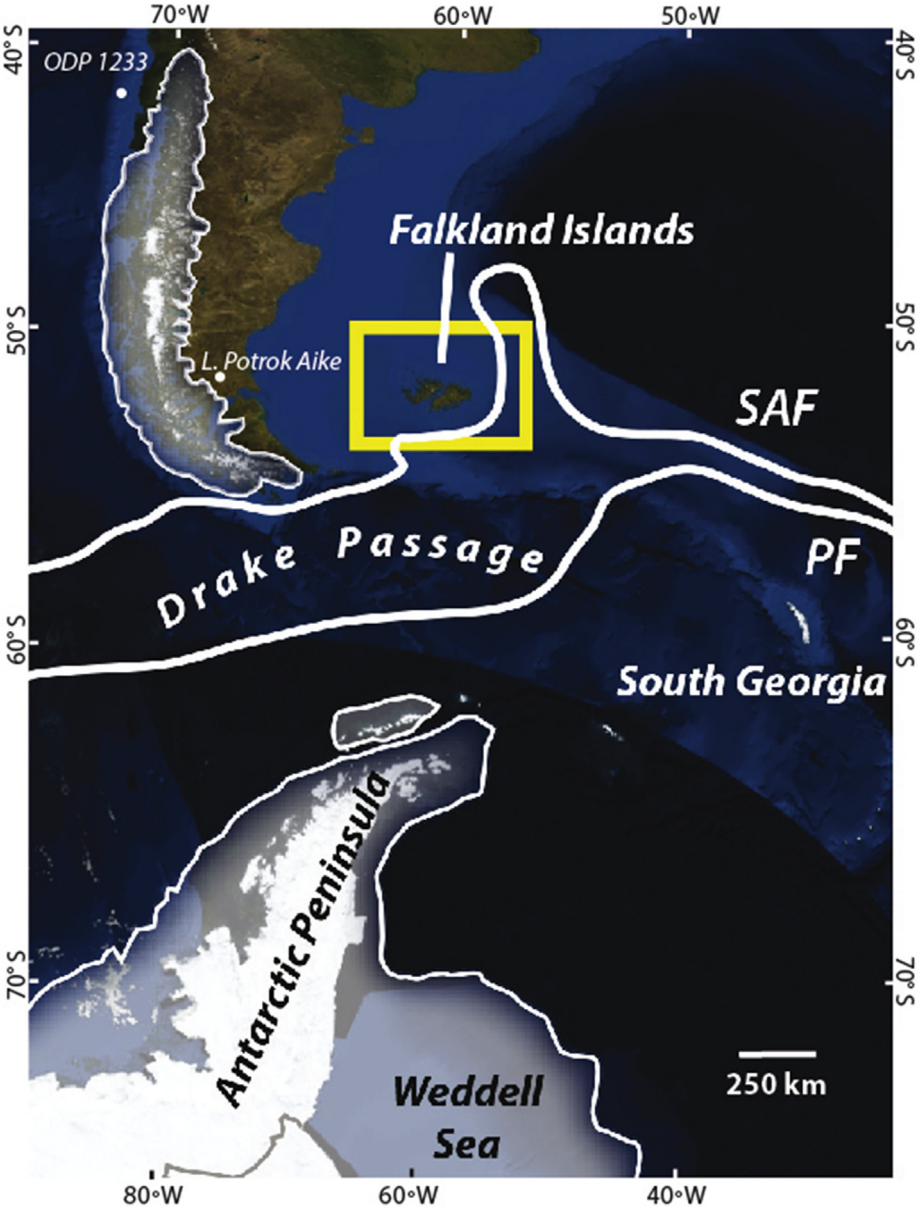

Fig. 1. Location of the field area (yellow box) in the context of the Southern Ocean and surrounding continents. White lines denote frontal boundaries (PF=Polar Front, SAF=Subantarctic Front). White shading outlines ice masses in South America and Antarctica during the last glacial maximum (LGM) (Caldenius, 1932; Denton and Hughes, 2002). Base imagery is from Google Earth. (For interpretation of the references to color in this figure legend, the reader is referred to the Web version of this article.)

Antarctic Circumpolar Current, with the upper 300 m water layer consisting of the Subantarctic Surface Water and the deeper layers occupied by Antarctic Intermediate Water (Peterson and Whitworth, 1989). The islands lie in the path of the Southern Westerlies, the dominant wind system in the mid-latitudes, the position of which has been linked repeatedly with episodes of climate change (i.e., Anderson et al., 2009; Denton et al., 2010; Björck et al., 2012; Fletcher and Moreno, 2012; Buizert et al., 2018). Our work was designed to answer three specific questions. First, when was the local last glacial maximum on East Falkland, as determined by glacial extent? What was its duration and structure? What was the relationship (if any) between glaciation and orbital variation?

2. Background on the Falkland Islands

The Falkland Islands (52° S) lie in the zone of the Southern Westerlies and thus winds and storm systems are overwhelmingly from the west (Upton and Shaw, 2002). The islands are relatively arid, with the centrally located Mt. Pleasant weather station receiving only 576 ± 103 mm per year near sea level (1992–2014). Observations suggest greater (but unquantified) precipitation and humidity at higher elevations. Mean annual temperature at Mt. Pleasant is 6.7 ± 0.3 C (Lister and Jones, 2015). The landscape is treeless and dominated by grasses, sedges, and bogs, as well as nearly ubiquitous 'stone runs', which are periglacial features. The abundant periglacial features on the islands appear to have a long history (e.g., Hansom et al., 2008; Wilson et al., 2008).

There are no glaciers in the Falkland Islands today; snow on the highest peaks survives in drifted patches into early summer during some years. However, the existence of former glaciers on the highest peaks of both East and West Falkland has been known for decades. From a study of geomorphology, Clapperton (1971), Clapperton and Sugden (1976), and subsequently Roberts (1984) identified several cirques and nivation basins, as well as moraines of limited extent, on both major islands (East and West Falkland). Although undated, the features were presumed to date to the Quaternary.

We focus here on Mt. Usborne (705 m), the highest peak on East Falkland (Fig. 2). The mountain is part of a long, roughly east-west trending, quartzite highland that cuts across the center of the island, known as the Wickham Heights. The peak itself is hardly distinguishable from a summit tableland. Five cirques, each supporting a tarn, are cut into the north slope and are fringed by large, composite moraines.

3. Methods

We mapped the field area by extensive traverse on foot aided by half-meter World View and vertical and oblique drone imagery, which we obtained using a DJI Phantom 3A drone. Because of the composite nature of the moraines, separation of distinct drift units was difficult. We based our units on the presence of subtle individual moraine crests visible by eye either on the ground or in drone imagery. Mapped drift units relate to surficial deposits and subdued moraine crests, which likely make up only the upper portions of very large composite landforms. We almost certainly have underestimated the number of glacial events represented by the composite moraines. Correlation of drift units among cirques was based on position of moraines in each basin. Final correlations also had to be consistent with the exposure-age chronology.

We selected large, stable, isolated boulders unassociated with visible periglacial disturbance or rock accumulations for ^{10}Be exposure age dating. Suitable boulders were uncommon, and the

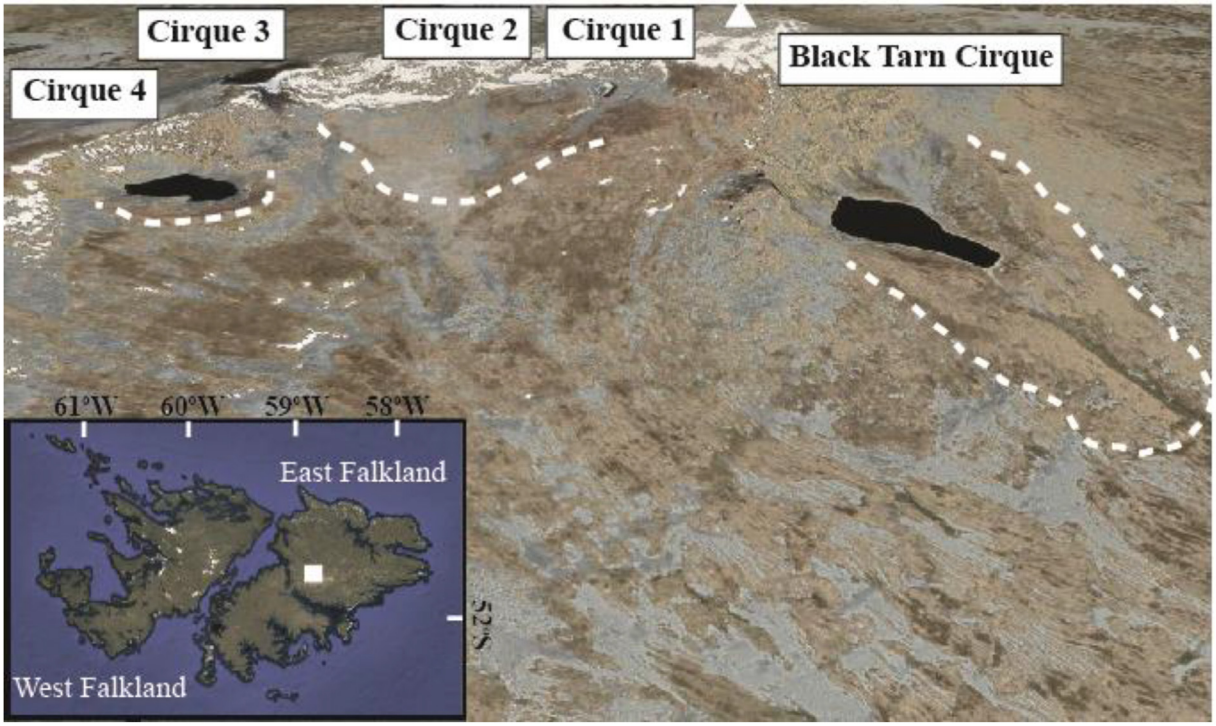

Fig. 2. Oblique aerial view of the northeast side of Mount Usborne with view to the southwest, showing the studied locations. White dashed lines mark the approximate outer limit of observed glacial drift. Triangle marks the summit. Inset map shows location of Mt. Usborne within the Falkland Islands. For reference, the Black Tarn is approximately 0.5 km long. Base images are from Google Earth.

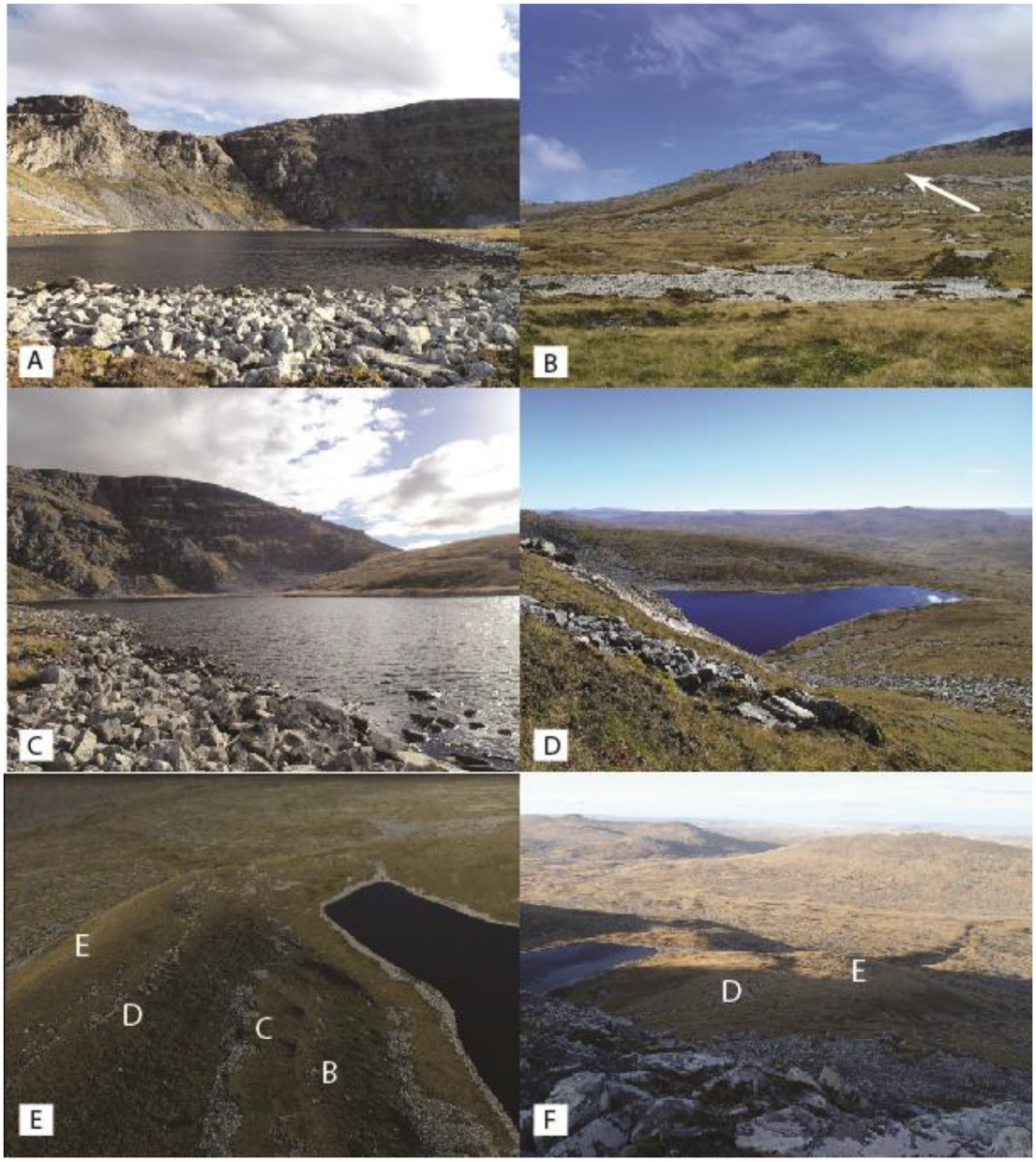

Fig. 3. Images of Black Tarn Cirque and moraines. A. View southwest across the Black Tarn toward the headwall; B. Approaching the moraines (white arrow) from the northwest looking southeast; C. View toward the headwall (southwest) and left lateral moraines; D. View to the northwest from the headwall, showing the tarn and moraines; E. Drone imagery of the left-lateral region with view to the north. Moraine crests are marked with white letters; F. Right-lateral deposits, with two principal units marked in white letters; view is to the northwest.

age of some features is assessed with only two dates. We extracted samples with hammer and chisel and recorded positions with a hand-held GPS with an averaging function to improve precision. We estimate vertical accuracy at ~5 m. Selected samples were reduced to clean quartz by a series of weak HF etches. Purity was confirmed by ICP-OES. We dissolved 10–15 g of pure quartz in concentrated HF and processed them using standard ion exchange chromatography modified from Ditchburn and Whitehead (1994) at the University of Maine Cosmogenic Isotope Laboratory (https://umaine.edu/earthclimate/research/glacial-geology-and-geochronology-research-group/cosmogenicisotope/). Beryllium was precipitated as hydroxide, combusted, mixed with niobium and packed into cathodes, which were analyzed at Lawrence Livermore National Laboratory. We calculated ages using the former CRONUS online calculator of Balco et al. (2008; v.3), the New Zealand production rate (Putnam et al., 2010), and Lal (1991)/Stone (2000) scaling. We chose the New Zealand rate over the geographically closer but indistinguishable Patagonian value of Kaplan et al. (2011), because the New Zealand rate has better precision and comes from a site with elevation similar to that of our field area. Using the Patagonian rate would not materially affect our results (ages would be slightly less than 2% older). Per convention, all dates are presented with 1-sigma internal errors. Outliers were identified using chi-squared statistics at 2-sigma confidence level. We present the data in figures as probability distributions and use mean ages in the text for discussion purposes.

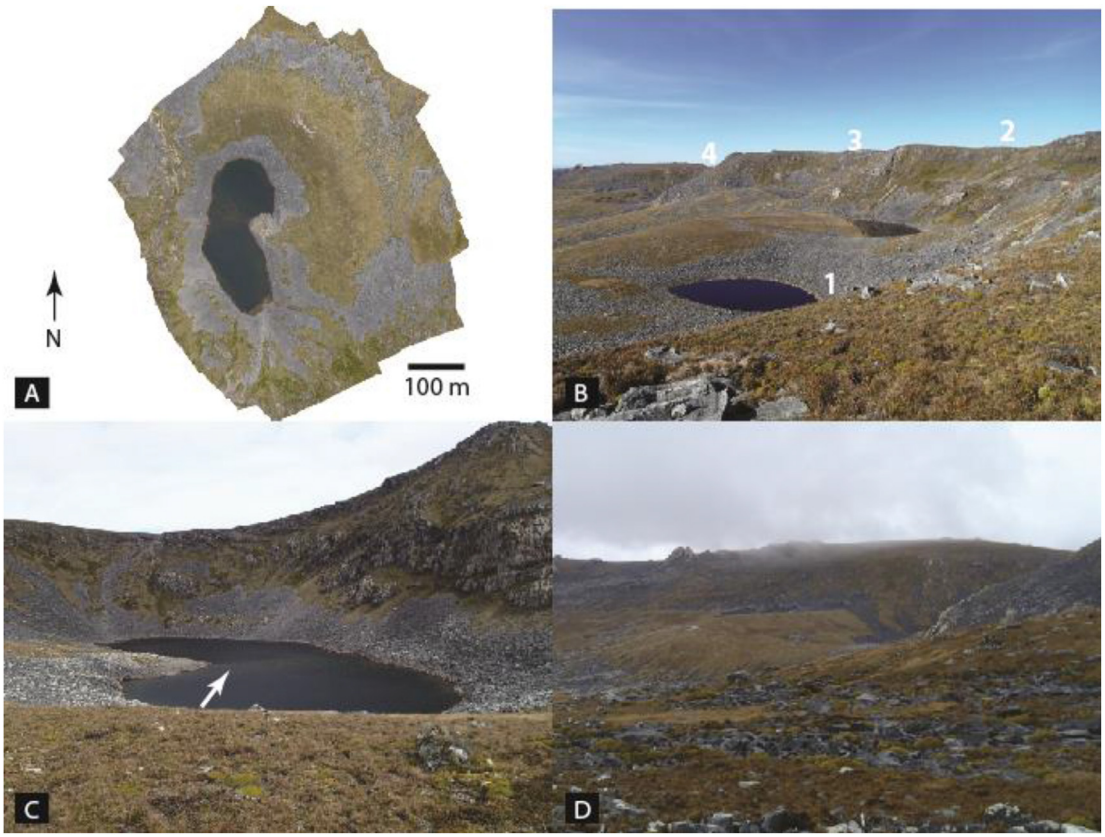

Fig. 4. Images of the upper cirques on Mt. Usborne. A. Orthorectified map of Cirque 4 from drone imagery. The image extends from the headwall (bottom edge of image) north to the edge of the large composite moraine. The moraine is clearly visible on the north and east sides of the lake. B. View to the east of the upper four cirques, labelled in white, taken from the slope west of Cirque 1. C. View of Cirque 4 to the southeast. The tarn is divided by a moraine, marked with an arrow. D. View of Cirque 4 moraine from the west.

4. Results

4.1. Surficial geomorphology

Five cirques on the northeast slope of Mt. Usborne afford the most striking evidence of glaciation on East Falkland (Clapperton, 1971). These cirques are floored at three different elevations. The largest, and the one with the most impressive headwall (130–250 m of near vertical relief), lies at ~385 m elevation and supports a lake known as the Black Tarn in an over deepened basin (Fig. 3). We refer to this as the Black Tarn Cirque, and it faces northeast. No other cirques of this elevation presently occur on Mt. Usborne.

The remainder of the cirques (named informally 1–4 from west to east) are grouped above a large basin southeast of the Black Tarn and are cut into the summit tableland (Fig. 4). Of these, Cirque 4 is at the lowest elevation (520 m) and is the easternmost. It has a distinct bowl shape and a steep headwall with ~100 m of relief. The cirque faces north-northwest. The remaining three cirques are smaller and at higher elevation, floored at ~600 m. Headwall relief decreases to the west, and all three high-elevation cirques face north.

Large (20–60 m of relief), broad, composite moraines flank all cirques on Mt. Usborne (Fig. 5). In some locations, multiple subtle crests can be discerned (particularly from the air). All glacial deposits appear to be constrained to within 1.25 km of the headwalls. We have not found unambiguous evidence for glaciation beyond the outer terminal moraines. Nor do there appear to be outwash deposits of the kind normally found in temperate regions. Rare exposures suggest that the moraines appear to consist of silty sandy diamicton and, although uncommon, striated stones are present.

The largest set of moraines occurs at the Black Tarn Cirque, where composite laterals rise as much as 50 m above the tarn (Figs. 3 and 5). At least four separate, subdued crests (designated Drifts B-E) can be seen in drone imagery and, in places, on the ground. Terminal moraines are subdued and have been cut by an outlet stream. A fan of colluviated drift (Drift F), possibly reworked older terminal moraines, extends as much as 0.5 km downslope of the clear ridges. A bowl filled with abundant lichen-free boulders occurs immediately below the headwall, banked against the left-lateral moraine. Based on the absence of lichens, this bowl likely supported a permanent snowbank at least periodically until Historical times and even now holds a snowbank into early summer.

The composite nature of the landforms is less visible at Cirque 4, where a single large moraine (~40 m of relief; Drift B) spans the basin mouth (Fig. 4). At least two colluviated recessional ridges occur on its proximal slope, and a distinct moraine (Drift A) divides the two basins of the tarn. The tarn itself is encircled by extensive deposits of loose, large boulders.

Moraines at Cirques 1–3 are broader and more degraded than those at the other two basins. Each basin has its own set of broad, vegetated “inner” moraines, located adjacent to the tarns (Drifts A-D). At Cirques 1 and 3 there also are distinct lines of unweathered boulders of uncertain origin that lie on top of the vegetated inner moraines. A very degraded, broad “outer” moraine (Drift E) extends as much as 0.4 km beyond the inner moraines and represents a time when ice from all three basins fed into a single ice mass.

The most striking landforms in the field area are not the moraines, but rather the ‘stone runs,’ ubiquitous boulder deposits that, in the Falkland Islands range from broad, rock-glacier-like features

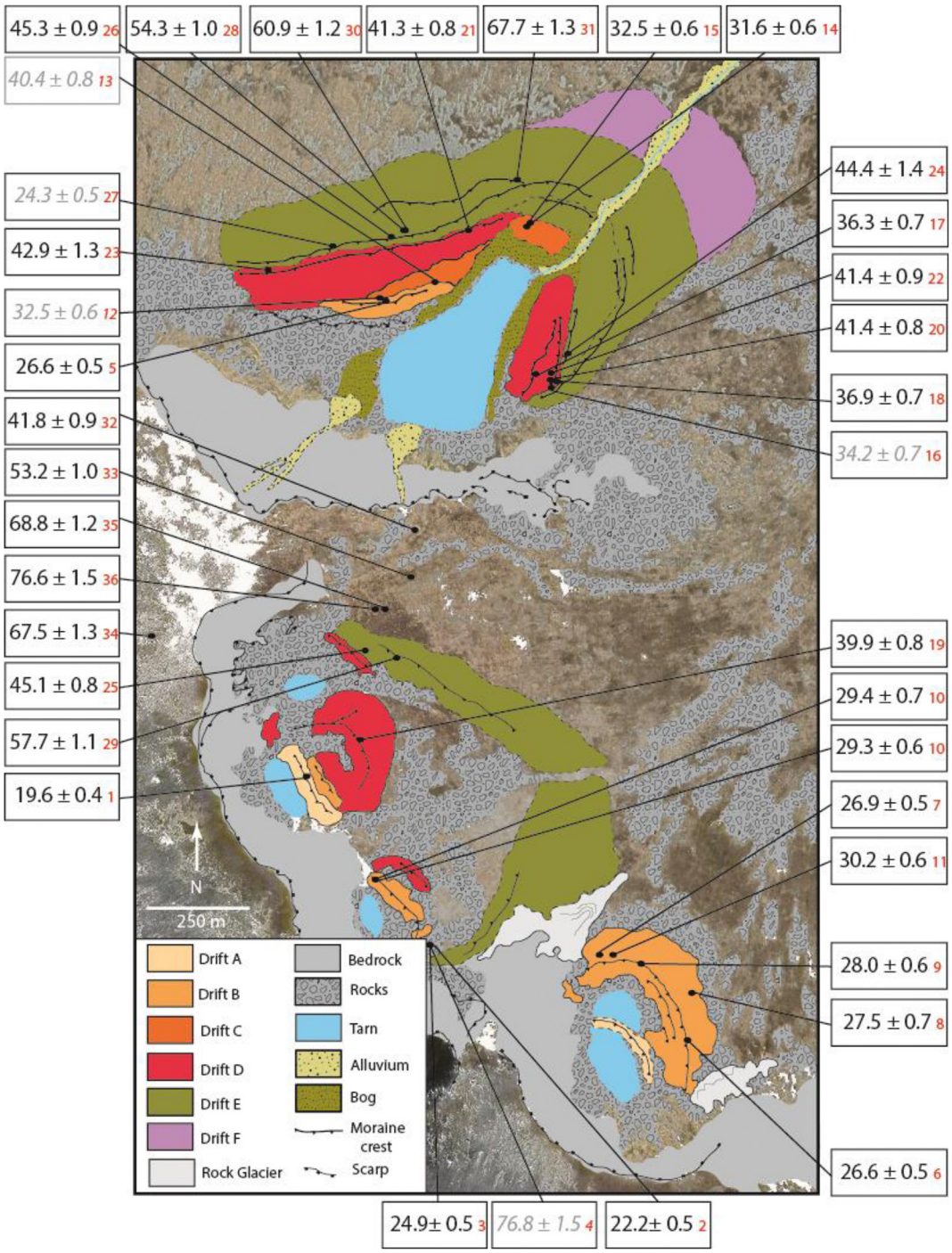

Fig. 5. Geomorphological map of deposits at Mt. Usborne. Subscripts after the dates (in ka) are keyed to Table 1. Dates in italicized gray text are considered outliers. Basins are, from north to south, the Black Tarn Cirque and Cirques 1 through 4.

to stone stripes to polygons and boulder-filled basins (Clark, 1972; Wilson et al., 2008). In addition to boulder depressions at the Black Tarn and at some of the higher cirques, there are several other prominent stone features in the field area, and the summit of Mt. Usborne displays felsenmeer and relict sorted polygons. Large blocks that occur distal to the outermost visible moraines near Cirque 1 (Fig. 6) may be of periglacial origin, although we cannot rule out the possibility that they were left by more extensive, older glaciation. They are not associated with any visible stone run and the slope angle is low.

4.2. Exposure ages

Thirty-seven ^{10}Be exposure ages constrain the late Quaternary history of Mt. Usborne and range from 19.6 to 76.8 ka (Table 1; Figs. 5–7). The data are largely internally consistent and in keeping with the geomorphology. However, three samples (BT-15-4; BT-15-8B; UBT-16-2) are significantly different from other ages on the same landforms and are discarded as geological outliers; they are not considered further. Two additional ages were identified as statistical outliers at the 2-sigma confidence level (BT-15-3; UBT-

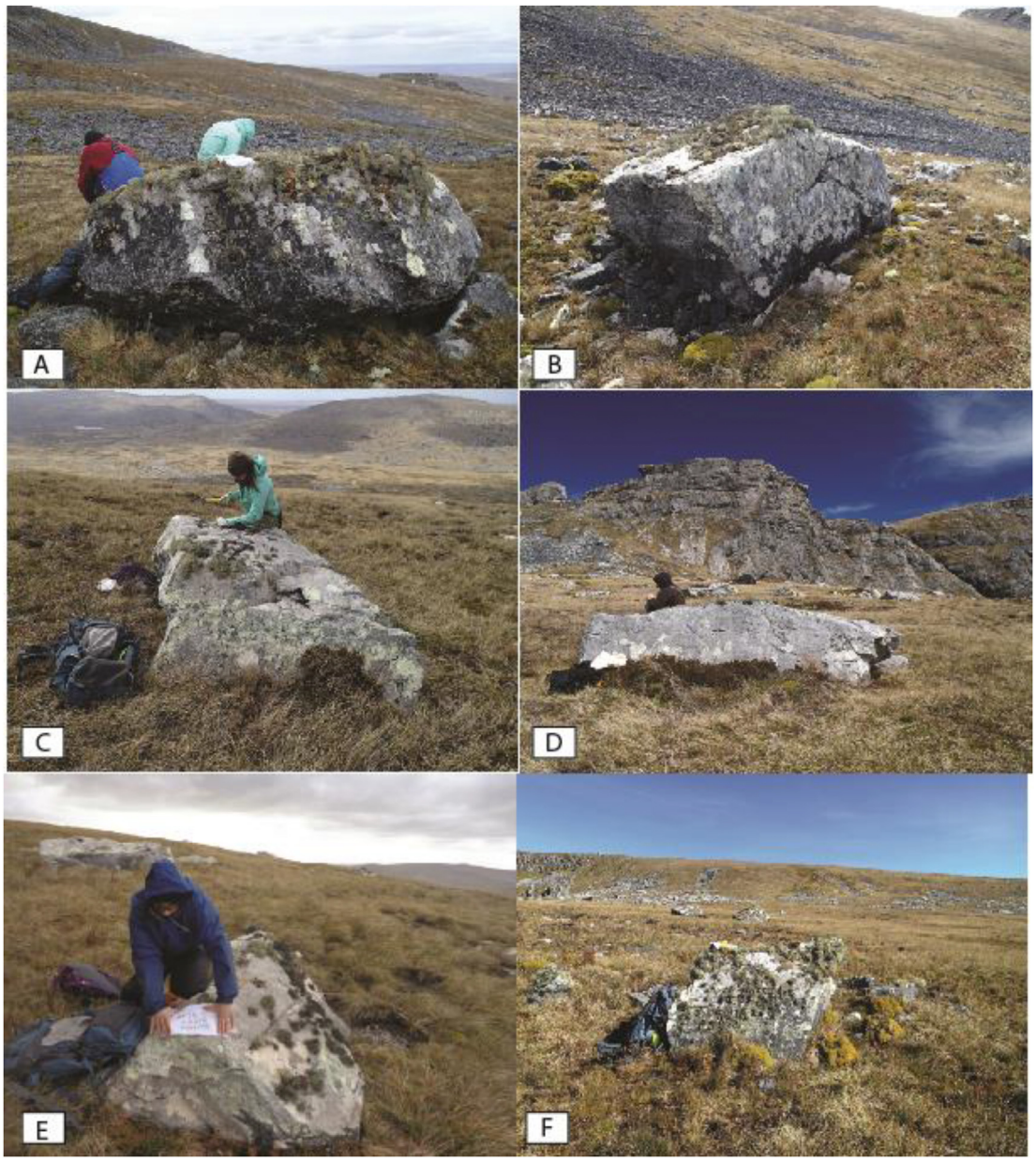

Fig. 6. Examples of sampled boulders on Mt. Usborne (see also Table 1). A. MTU-18-1 at Cirque 3. This sample is a replicate of BT-15-7; B. BT-15-13 on the large Cirque 4 moraine; C. BT-15-16 from the Black Tarn Cirque left lateral deposits; D. MU-13-1 from the right lateral deposits at the Black Tarn Cirque; E. BT-15-4 on the outer left lateral deposits of the Black Tarn Cirque; F. UBT-16-8, a block distal to visible moraines west of Cirque 1. UBT-16-7 is the left of the two large boulders in the distance.

16-4) and have been removed from the calculated mean ages. Our conclusions are unaffected by removal (or not) of these latter two outliers.

The oldest group of samples (n = 4) comes from summit felsenmeer (largely *in situ* fractured bedrock) and from large, possibly periglacial, blocks that litter the slope distal to the outermost visible moraines northwest of Cirque 1. Because these blocks may be of periglacial rather than glacial origin, we conservatively interpret the ages as total exposure time, rather than time since deglaciation. The blocks yield three ages ranging from 53.8 to 76.6 ka. The summit felsenmeer produced an age of 67.5 ka.

Dates from confirmed glacial deposits (n = 33; Fig. 7) are nearly all younger, although several overlap the ages of the blocks mentioned above. Five exposure ages of the oldest datable drift (E) at the Black Tarn Cirque range from 44.4 to 67.7 ka, with a sixth age of 24.3 ka considered to be an outlier (Fig. 7). In the right lateral area, Drift E displays at least two moraine crests, the inner of which has a boulder dated to 44.4 ka. Likewise, the innermost left-lateral crest displays a similar age of 45.3 ka. Two boulders distal to the innermost crest in the left lateral area yield ages of 54.3 and 60.9 ka. A sample on a yet more distal crest dates to 67.7 ka. Two additional ages of Drift E come from deposits at Cirque 1, where the inner sample dates to 45.1 ka and the outer sample is 57.7 ka. These data suggest at least two events produced Drift E, with the youngest, best-defined event forming the ice proximal part of the drift unit at 44.9 ± 0.3 ka (Fig. 7). Older ages on more distal parts of Drift E represent one or more marine oxygen isotope stage (MIS) 4 or older advances, the age(s) of which cannot be constrained tightly.

Eight dates constrain the age of Drift D and show a bimodal distribution (Fig. 7). At the Black Tarn Cirque, two dates from the

Table 1
Exposure-age data. All samples are referenced against 07KNSTD (Nishiizumi et al., 2007). Superscripts in the first column are keyed to the map in Fig. 5. Ages of inferred outliers are in italics and all ages are given with 1σ internal errors. Blank corrections averaged <2% and were propagated in quadrature. BT-15-7 and MTU-18-1 are two different samples of the same boulder and yield identical ages.

Sample	Location	Dimensions L x W x H (m)	Lat.	Long.	Elev. (m)	Thickness (cm)	Shielding	^{10}Be (at/g)	Error (at/g)	Age (yr BP)	Error (yr BP)
Drift A											
MTU-18-3[1]	Cirque 2	1.3 × 0.9 x 1.0	−51.6963	−58.8271	595	2.0	0.993754	1.46E+05	2.59E+03	19,590	350
BT-15-9[2]	Cirque 3	3.0 × 1.3 x 1.5	−51.6999	−58.8229	601	1.2	0.998634	1.68E+05	4.00E+03	22,180	530
BT-15-8A[3]	Cirque 3	3.0 × 2.3 x 1.5	−51.6999	−58.8229	601	3.0	0.987871	1.84E+05	3.69E+03	24,860	500
BT-15-8B[4]	Cirque 3	0.3 × 0.2 x 0.1	−51.6999	−58.8229	601	3.0	0.987871	5.60E+05	1.07E+04	*76,820*	*1500*
Drift B											
UBT-16-3[5]	Black Tarn	0.9 × 0.4 x 0.5	−51.6857	−58.8246	408	0.9	0.988261	1.68E+05	3.34E+03	26,630	530
BT-15-10[6]	Cirque 4	1.8 × 1.5 x 0.7	−51.702	−58.8142	560	1.6	0.996641	1.93E+05	3.64E+03	26,630	510
BT-15-13[7]	Cirque 4	3.0 × 2.0 x 1.3	−51.7002	−58.8172	546	3.5	0.995341	1.90E+05	3.13E+03	26,910	450
BT-15-11[8]	Cirque 4	2.0 × 1.0 x 1.0	−51.7008	−58.8150	561	2.8	0.997022	1.98E+05	4.98E+03	27,450	700
BT-15-12[9]	Cirque 4	2.0 × 1.0 x 1.0	−51.7004	−58.8157	552	1.0	0.997296	2.03E+05	4.48E+03	28,030	620
BT-15-7[10]	Cirque 3	3.0 × 2.5 x 1.3	−51.6987	−58.8244	601	1.9	0.990714	2.13E+05	5.31E+03	29,370	740
MTU-18-1[10]	Cirque 3	3.0 × 2.5 x 1.3	−51.6987	−58.8244	601	4.4	0.994958	2.15E+05	4.68E+03	29,320	640
BT-15-14[11]	Cirque 4	2.5 × 1.0 x 0.5	−51.7002	−58.8167	550	2.1	0.995341	2.16E+05	4.12E+03	30,170	580
UBT-16-4[12]	Black Tarn	1.1 × 0.6 x 0.3	−51.6857	−58.8249	408	1.7	0.985380	2.03E+05	3.91E+03	*32,470*	*630*
UBT-16-2[13]	Black Tarn	1.6 × 1.1 x 0.4	−51.6853	−58.8229	401	5.2	0.988261	2.47E+05	4.99E+03	*40,350*	*820*
Drift C											
BT-15-15[14]	Black Tarn	2.0 × 0.5 x 0.7	−51.6841	−58.8195	386	2.1	0.991172	1.94E+05	3.73E+03	31,640	610
BT-15-18[15]	Black Tarn	2.0 × 3.0 x 1.5	−51.6842	−58.8194	384	1.4	0.996695	2.02E+05	3.93E+03	32,530	640
Drift D (young)											
BT-15-3[16]	Black Tarn	1.7 × 1.0 x 1.3	−51.6877	−58.8186	432	1.1	0.990982	2.21E+05	4.61E+03	*34,170*	*720*
MTU-18-27[17]	Black Tarn	2.1 × 2.2 x 1.4	−51.6874	−58.8193	412	2.3	0.991385	2.28E+05	4.36E+03	36,310	700
BT-15-2[18]	Black Tarn	2.7 × 2.3 x 1.0	−51.6876	−58.8185	432	2.2	0.992032	2.36E+05	4.56E+03	36,870	720
Drift D (old)											
MTU-18-5[19]	Cirque 2	3.0 × 0.8 x 1.3	−51.6954	−58.8254	602	2.1	0.998388	2.99E+05	5.66E+03	39,940	760
BT-15-1[20]	Black Tarn	2.0 × 2.5 x 0.7	−51.6876	−58.8186	432	1.8	0.989943	2.65E+05	4.93E+03	41,380	780
BT-15-6[21]	Black Tarn	2.2 × 0.6 x 0.9	−51.6842	−58.8224	415	2.2	0.998634	2.62E+05	4.95E+03	41,290	790
MTU-18-28[22]	Black Tarn	1.9 × 0.9 x 0.8	−51.6874	−58.8187	421	2.5	0.992959	2.62E+05	5.32E+03	41,430	850
MU-13-3[23]	Black Tarn	2.0 × 1.5 x 1.0	−51.6851	−58.8286	448	1.0	0.995525	2.82E+05	8.30E+03	42,940	1280
Drift E (young)											
MU-13-1[24]	Black Tarn	2.5 × 1.5 x 1.5	−51.6870	−58.8181	416	3.3	0.99802	2.79E+05	8.57E+03	44,430	1380
UBT-16-6[25]	Cirque 1	1.3 × 1.0 x 0.5	−51.6936	−58.8249	598	1.4	0.993163	3.37E+05	5.50E+03	45,110	750
MTU-18-29[26]	Black Tarn	2.4 × 1.6 x 0.6	−51.6843	−58.8246	429	3.8	0.997978	2.86E+05	5.32E+03	45,260	850
Drift E (old)											
BT-15-4[27]	Black Tarn	1.3 × 1.3 x 0.3	−51.6845	−58.8262	441	2.9	0.995945	1.57E+05	3.31E+03	*24,270*	*520*
MU-13-2[28]	Black Tarn	2.5 × 1.5 x 1.0	−51.6843	−58.8240	424	2.0	0.996832	3.46E+05	6.42E+03	54,300	1020
UBT-16-9[29]	Cirque 1	3.0 × 1.5 x 1.2	−51.6938	−58.8239	592	1.7	0.998634	4.28E+05	8.08E+03	57,680	1110
BT-15-5[30]	Black Tarn	2.3 × 0.7 x 0.5	−51.6843	−58.8240	431	2.6	0.997606	3.88E+05	7.64E+03	60,880	1220
BT-15-16[31]	Black Tarn	1.8 × 1.3 x 0.8	−51.6831	−58.8199	381	0.8	0.998752	4.18E+05	7.95E+03	67,680	1310
Erratics and Blocks											
UBT-16-14[32]	Black Tarn	0.2 × 0.2 x 0.1	−51.691	−58.8232	565	4.8	0.998839	2.96E+05	5.98E+03	41,790	850
UBT-16-12[33]	N of Cirque 1	1.3 × 1.1 x 0.9	−51.692	−58.8234	574	1.5	0.999819	3.93E+05	7.48E+03	53,220	1030
UBT-16-5[34]	Summit	3.0 × 1.2 x 0.7	−51.6932	−58.8320	690	1.0	1	5.49E+05	1.04E+04	67,480	1300
UBT-16-8[35]	N of Cirque 1	1.9 × 1.2 x 1.1	−51.6927	−58.8243	589	2.4	0.999208	5.05E+05	8.30E+03	68,810	1150
UBT-16-7[36]	N of Cirque 1	2.2 × 1.4 x 1.2	−51.6927	−58.8246	594	1.0	0.999208	5.70E+05	1.12E+04	76,570	1530

left lateral moraine are 42.9 and 41.3 ka. Two similar (41.4, 41.4 ka), as well as three younger (36.9, 36.3, 34.2 ka) ages, come from the right lateral landform. The eighth date, from a correlative drift at Cirque 2, is 39.9 ka. A perched erratic at the top of the Black Tarn headwall yielded a similar age of 41.8 ka. These two populations of ages suggest expanded glaciers at 41.4 ± 0.5 ka and 36.6 ± 0.3 ka (with removal of younger statistical outlier of ~34 ka).

Two adjacent boulders on Drift C, which forms a terminal moraine at the end of the Black Tarn, yield ages of 32.5 and 31.6 ka, producing a mean age of 32.1 ± 0.4 ka (Figs. 5 and 7). The coeval lateral moraines are not well preserved, and there are no other suitable boulders for dating.

Drift B yields 10 dates ranging from 26.6 to 40.4 ka, with most dating to ~27–28 ka (Fig. 8). Drift B is dated best at Cirque 4, where it forms a distinct moraine with five ages ranging from 26.6 to 30.2 ka. A boulder on a similar moraine at Cirque 3 (dated twice) yields ages of 29.3 and 29.4 ka. The innermost moraine at the Black Tarn Cirque, thought to be part of Drift B based on its position, terminates before the end of the lake inboard of Drift C and produced three widely scattered ages of 26.6, 32.5, and 40.4 ka. We consider the two older ages to be outliers, possibly derived from drifts C (~32 ka) and D (~41 ka), against which Drift B is banked. We tentatively propose that the younger age, 26.6 ka, dates Drift B at the Black Tarn Cirque, but cannot be certain. The overall distribution of ages from Drift B at all sites produces a prominent peak at 27.9 ± 0.5 ka, when the two older outliers at the Black Tarn are excluded. The most precise age of Drift B from a single landform comes from Cirque 4, where it yields an age of 27.3 ± 0.3 ka (one older outlier removed).

Drift A (Fig. 8) occurs only at the higher-elevation cirques and is dated only at Cirques 2 and 3. At Cirque 2, a single age from a boulder on the innermost moraine is 19.6 ka. Two samples on rock deposits on the innermost moraine at Cirque 3 are 22.2 and 24.9 ka. A third – a perched erratic in the same location – is 76.8 ka and is designated an outlier. With three samples ranging from 19.6 to 24.9 ka, a mean age is not possible.

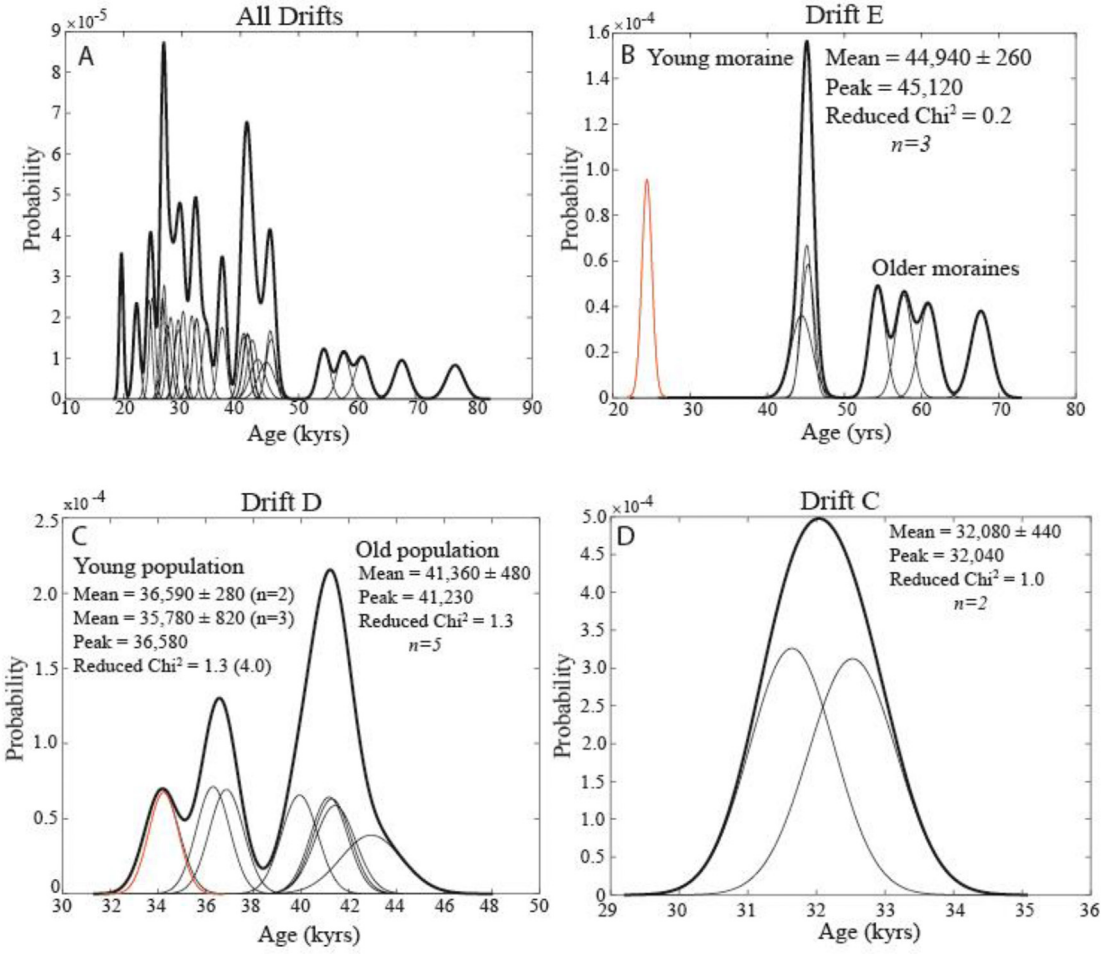

Fig. 7. Probability distributions of exposure ages from Mt. Usborne. A. Ages from all glacial deposits. B. Age of Drift E. Mean age shown (±1s s.e.) is for the youngest moraine. No mean is possible for the older samples. Sample in red is considered an outlier, because it is significantly younger than all other ages. C. Drift D, showing the young and old populations. Sample in red is considered a statistical outlier; mean ages with and without its inclusion are shown. D. Data for Drift C.

5. Discussion

5.1. Extent and timing of glaciation on Mt. Usborne

Our work bears out previous suggestions that glaciation in the Falkland Islands has been of limited extent (Clapperton, 1971; Clapperton and Sugden, 1976; Sugden and Clapperton, 1977; Roberts, 1984; Wilson et al., 2008). All deposits of clear glacial origin on Mt. Usborne are within 1.25 km (and commonly < 1 km) of the headwalls of present-day cirques. Thus, ELA depression was never sufficient, at least within the constraints afforded by the preserved glacial deposits, to cause widespread glaciation of East Falkland.

The oldest ages obtained from Mt. Usborne come from the outermost preserved moraines, from blocks distal to the outer moraines at Cirque 1, and from summit felsenmeer. These all date to MIS 4, a time of significant temperature depression (e.g., Jouzel et al., 2007; De Deckker et al., 2019) and glacial advance (e.g., Schaefer et al., 2015) in parts of the Southern Hemisphere, although we acknowledge that these dates are limited in number, show considerable scatter, and may afford only minimum ages. The position of moraines with MIS 4 ages indicates that ice advance during MIS 4 or potentially during an earlier time period was larger than during the global LGMat ~19–26.5 ka.

The oldest ages obtained by this study, whether from glacial or periglacial features, are from the last glacial period. None of the dates is from the penultimate glaciation (i.e., MIS 6) or earlier. There is not yet any direct (dated) evidence of glaciation in the Falkland Islands prior to the late Pleistocene, although we suspect such evidence probably is buried deep within the composite moraines at Mt. Usborne. If so, the extent of all Quaternary glaciations must have fallen within the approximate limits of that of the last ice age.

We anticipated that the summit age of 67.5 ka would be much older. End-member interpretations of the age are either that a fresh surface was uncovered by ice early in MIS 4 and has ~67 ka of exposure since then or that it represents the sum of several periods of exposure separated by long periods of burial by ice. If the former, it would indicate substantial erosion (glacial or otherwise) to remove all evidence of exposure during the preceding MIS 5, something that at face value, seems unlikely. For example, any ice cap on the summit plateau would probably have been thin and non-erosive, making glacial erosion improbable. The second end-member hypothesis would imply long periods of snow cover on the summit with only brief periods of ice-free conditions to build up nuclides. While we favor this latter hypothesis, testing it is beyond the current scope of this project.

Overall, the most striking feature of our data is that maximum conditions of the last glaciation probably were reached during MIS 4 and were repeated periodically between at least ~20–45 ka. At least six millennial-scale ice advances at ~19–24 ka, 27.3, 32.1, 36.6,

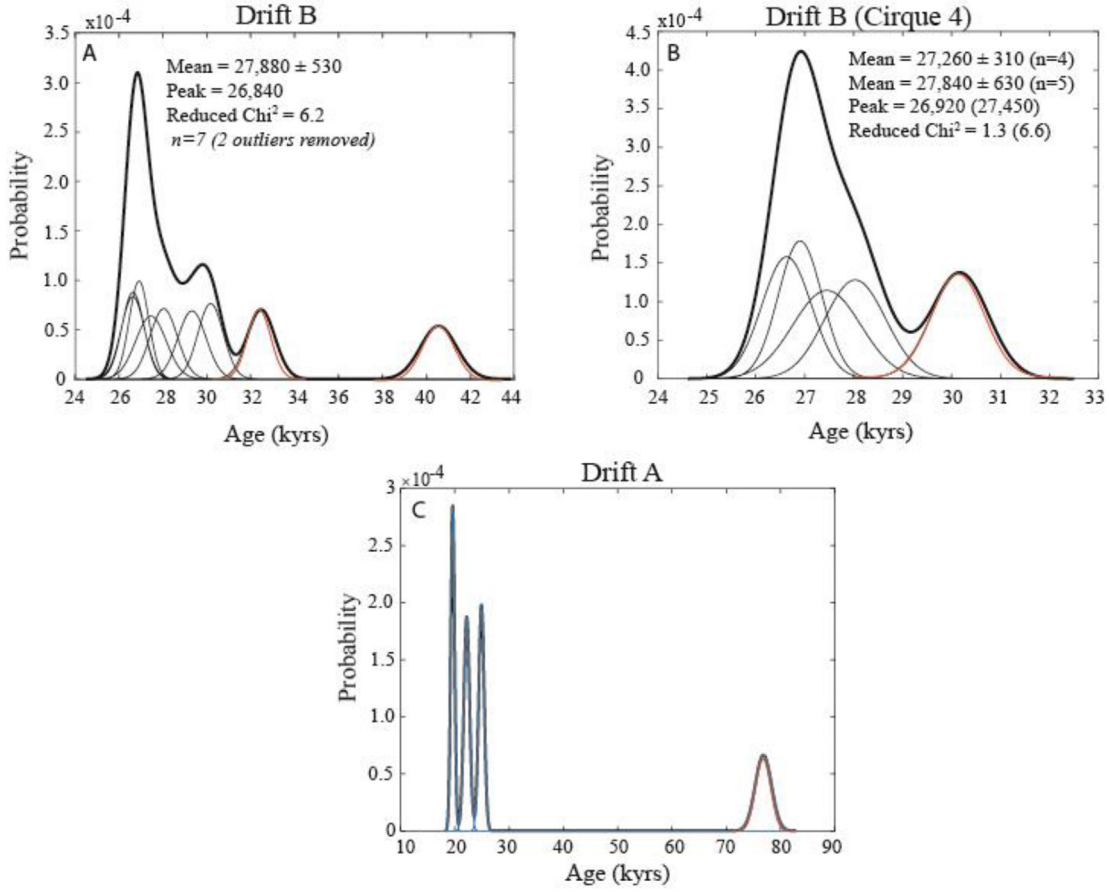

Fig. 8. Probability distributions of ages from the younger drifts on Mt. Usborne. A. Ages from all Drift B moraines. Those samples in red are designated outliers. B. Drift B from Cirque 4, the location of the best-preserved and best-dated moraine of this age. One sample (red) is designated an outlier. We use the age from Cirque 4 when referring to Drift B in the text. C. Drift A ages. Sample in red is considered to be an outlier, because it is much older than the remaining ages. Samples range from 19 to 24 ka and, because of that range, no mean age is possible.

41.4, and 44.9 ka punctuate the glacial record after MIS 4. The global LGM does not stand out among these events. Earlier ice expansions appear to have been more extensive than later fluctuations. Some size reduction could be attributed to large moraine walls containing subsequent glacier extent. However, younger moraines are also less extensive at sites without large moraine walls, and the only conclusive evidence of the youngest glacial event at 19–24 ka is at the highest-elevation cirques, where ice might be expected to persist the longest. Moreover, large moraine walls would promote snow drifting, which we consider to be an important component of the total glacier mass balance. Thus, the development of such landforms could lead to greater ice extent, not less. We conclude that the millennial pattern of ice expansion was superimposed on an overall reduction in ice volume from at least ~45 ka to the end of MIS 2.

5.2. Long-term trends and their possible cause

Our data show that maximum or near-maximum ice extent was reached repeatedly over tens of thousands of years (Figs. 5 and 9) regardless of orbital state, indicating a lack of correspondence between local insolation and glacier variation. Such a conclusion also has been reached for glaciers in the Southern Alps of New Zealand (Kelley et al., 2014; Doughty et al., 2015; Schaefer et al., 2015, Strand et al., 2019). Moreover, such a protracted "LGM" period, starting as early as 45 ka, also has been noted for South America (Darvill et al., 2016), although no one area shows evidence (yet) of the entire sequence of events. Our data do not support the idea that the maximum of the Southern Hemisphere glaciation was at 28 ka and driven by obliquity (Fogwill et al., 2015). While ice in the Falkland Islands did advance at roughly 28 ka, this expansion was one of several similar events and was not characterized by unusual or even maximum ice extent.

The Mt. Usborne data support the idea of gradual contraction of the maximum ice limit over time during each of the millennial events. By 45 ka and likely by MIS 4, glaciers on Mt. Usborne were more extensive than at 19–24 ka, when ice was largely gone from the mountain. Reduction in ice volume from 19 to 45 ka does not appear to have been significant in New Zealand, where moraines dating to these time periods are in proximity but may have been large in parts of Patagonia (e.g. Darvill et al., 2017; Davies et al., 2020). For example, Garcia et al. (2018) suggested that maximum ice extent of the Torres del Paine and Ultima Esperanza lobes, which lie at approximately the same latitude as the Falkland Islands, occurred by ~48 ka, and glaciers were significantly smaller by ~21 ka. If our ages for the outer moraines are reasonably correct, then ice volume also was larger in MIS 4. Some mid-latitude marine paleoclimate records suggest that MIS 4 may have been as cold or colder than MIS 2 (Kaiser et al., 2005; Barker and Diz, 2014; De Deckker et al., 2019).

The underlying cause of this ice reduction, if indeed it proves to be a widespread pattern, is key, because it highlights an important, but unidentified, secondary mechanism at work in some sectors of the Southern Hemisphere during the last glaciation. This

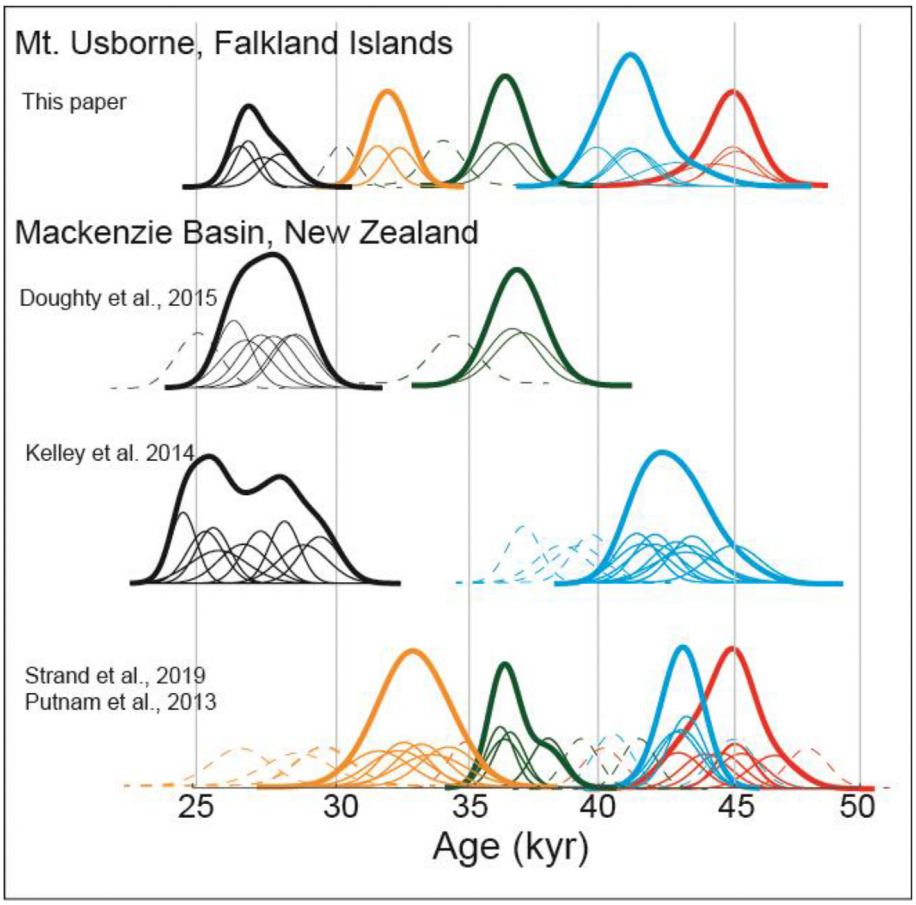

Fig. 9. Comparison of Mt. Usborne and Mackenzie Basin (New Zealand) cosmogenic isotope data. Each summed probability curve dates a particular moraine or drift. Curves are color-coded for comparison. Outliers are shown as dashed curves. Both data sets were calculated in the same manner (i.e., production rate, scaling, statistical protocol for outliers), which may result in a slightly different age than that suggested by the original authors. All New Zealand data are from the Pukaki lobe with the exception of a 33 ka peak (bottom panel) from a moraine at Lake Ohau (Putnam et al., 2013b). (For interpretation of the references to color in this figure legend, the reader is referred to the Web version of this article.)

mechanism would have caused glacier snowlines to rise gradually despite regional evidence (i.e., WAIS Divide ice core; Fig. 10) for cooling over the same time period. One possible contributing factor to ice extent being greater at 45 ka than at 20 ka despite cooling climate is the accompanying northward migration of the Southern Hemisphere westerlies, likely working in concert with Southern Ocean sea ice. During the LGM, the westerlies are thought to have lain well north of their present position, although there is little certainty as to how early in the glaciation they achieved this position. Lake-water oxygen isotopes at Laguna Potrok Aike on the South American mainland have been interpreted as indicating weak (northward-shifted) westerlies at approximately the same latitude as the Falkland Islands from 21ka to 26 ka, the beginning of their record (Zhu et al., 2014). Surface level of the same lake, which extends farther back in time (Zolitschka et al., 2013, Fig. 10), does not afford unambiguous evidence of the position of the westerlies, as lake level can be influenced not only by precipitation, but also wind-driven evaporation and humidity. Theoretically, progressive northward shift of the westerlies, linked with expanding Southern Ocean sea ice (i.e., Toggweiler et al., 2006; Esper and Gersonde, 2014a,b), could have reduced precipitation greatly at the latitude of the Falkland Islands, leading to a cold, dry environment that caused minor reduction in glacier extent over time (see also Fogwill et al., 2015). Testing this hypothesis awaits more detailed westerlies and sea-ice reconstructions, as well as better constraints on the spatial distribution of sites with decreasing glacial ice extent through MIS 4-MIS 2.

5.3. Millennial pattern

The Mt. Usborne record shows a distinct, millennial-scale rhythm of glacier expansion and contraction, which we compare here to mountain-glacier records from the Mackenzie Basin of the New Zealand Southern Alps. We choose this region for comparison because it exhibits the most comprehensively dated glacial sequence in the Southern Hemisphere. Moreover, samples from the Mackenzie basin were collected and analyzed using the same protocols that we employed at Mt. Usborne, ensuring that any similarities or differences are due to geologic and not analytical differences. One of the peaks described below, that at 26–27 ka, is reasonably well-documented in adjacent South America (Darvill et al., 2016). However, the older part of the South American record awaits further work before detailed comparisons can be made with the Mt. Usborne data.

Despite a possible difference in long-term trend of glacier extent, there is a resemblance between the Mt. Usborne and New Zealand records at a millennial timescale (Fig. 9). In every case, glacial expansion at Mt. Usborne is mirrored by that in New Zealand, suggesting a common southern mid-latitude glacier signal. Between ~27 and ~45 ka, expansions on Mt. Usborne occurred, on average, about every 4000 years. These glacier expansions also occur in periods between Northern Hemisphere Heinrich Stadials

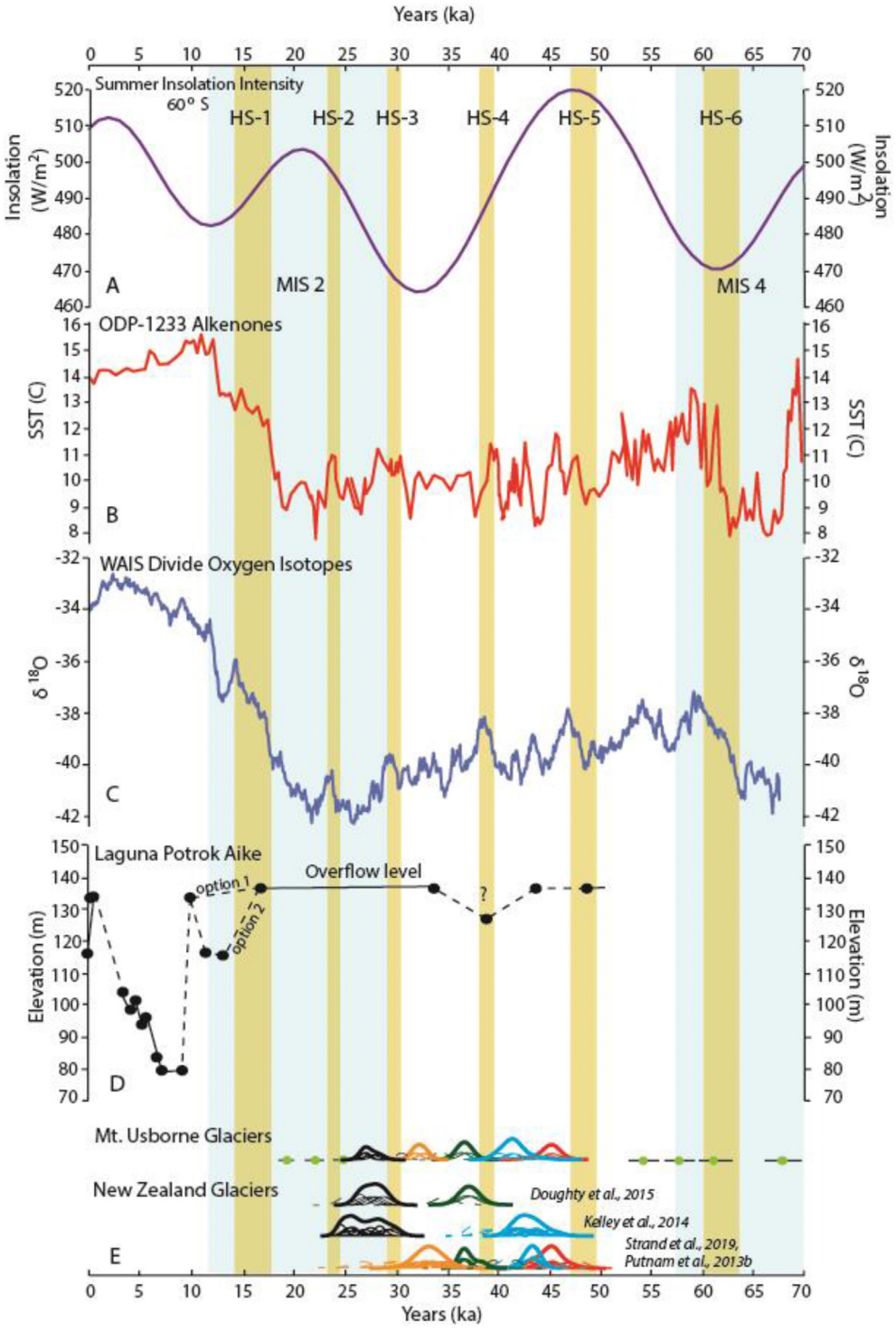

Fig. 10. Comparison of Mt. Usborne moraine data with other Southern Hemisphere climate proxies, including: A. Summer insolation intensity; B. ODP Site 1233 sea-surface temperatures derived from alkenones offshore of Chile (Kaiser et al., 2005); C. oxygen isotope records from WAIS Divide ice core, Antarctica (WAIS Divide Project Members, 2013, 2015); D. Lake-level record from Laguna Potrok Aike in South America (Zolitschka et al., 2013); E. Mt. Usborne, Falkland Islands and Mackenzie Basin, New Zealand mountain-glacier cosmogenic isotope data with similar-aged peaks color coded. Mt. Usborne data include probability curves for those drifts with sufficient data to produce a coherent age; other data are shown as points with 1-sigma error bars. New Zealand data are from Putnam et al. (2013b; 33 ka peak); Kelley et al. (2014); Doughty et al. (2015); and Strand et al. (2019). Gold bars show Heinrich Stadials (Wang et al., 2001, 2008; Cheng et al., 2009). Blue shading indicates marine oxygen isotope (MIS) stages 2 and 4 (Lisiecki and Raymo, 2005). (For interpretation of the references to color in this figure legend, the reader is referred to the Web version of this article.)

(HS) to such an extent that the interhemispheric linkage between these events must be more than coincidental. Glacier retreat on Mt. Usborne during Heinrich Stadials indicates warming of the South Atlantic region. This may reflect southward shifting of the westerlies, which would have allowed warm, northern air masses to penetrate the South Atlantic region. This atmospheric warming is

recorded at WAIS Divide in Antarctica, at least for Heinrich Stadials 0 through 4 (Fig. 10; WAIS Divide Project Members, 2013, 2015). Such a shift in the position of the westerlies, accompanied by southward movement of the subtropical and subantarctic ocean fronts, has been proposed as the cause of southern mid-latitude warming and glacier retreat during HS 1 (Anderson et al., 2009; Denton et al., 2010) and possibly during earlier Heinrich Stadials (i.e, De Deckker et al., 2012). However, unlike HS 1, which ushered in the ice-age termination, these earlier periods of warming and glacier retreat reverted back to glacial conditions, probably because the westerlies returned to their glacial position to the north and cold air masses once again prevailed in the region.

Our work affords the first detailed record of inter-Heinrich stadial glacier expansions in the southern mid-latitudes of the western hemisphere from 45–19 ka. It also confirms the wide geographic extent of these climate oscillations documented in New Zealand glacier records (e.g., Doughty et al., 2015; Strand et al., 2019), Antarctic Ice Cores (e.g., WAIS Divide Project Members, 2015), and, to some extent, in marine records (e.g., Kaiser et al., 2005; De Deckker et al., 2012; Barker and Diz, 2014) and pollen (e.g., Heusser et al., 1999). In addition, we note that there are more glacial advances at Mt. Usborne and in New Zealand than defined Heinrich Stadials. For example, two expansions occur between HS-3 and HS-4, with the same being true for most other examined Heinrich interstadials. Thus, the records also show a millennial pulsebeat that occurs on a shorter timescale than Heinrich Stadials and indicates additional complexity. This work supports the idea that an underlying millennial-scale periodicity drives climate fluctuations and only occasionally produces a Heinrich Stadial.

6. Conclusions

We present the first cosmogenic exposure ages for moraines on Mt. Usborne, East Falkland. These data show that glaciers reached their maximum extent of the last glacial period by 45 ka and possibly by MIS 4. Ice periodically returned to near-maximum extent until at least ~19 ka.

The data suggest gradual reduction in ice extent from 45 ka to ~19 ka on Mt. Usborne. The reason(s) for this minor reduction in the face of cooling climate is unclear but may relate to a drop in accumulation linked to a northern position of the westerlies and/or increased sea-ice extent, both of which would have reduced the frequency of moisture-bearing storms in the Falkland Islands.

Glaciers on Mt. Usborne fluctuated on a millennial timescale at a timing very similar to that documented for the Southern Alps of New Zealand. Expansions occurred between Northern Hemisphere Heinrich Stadials, although also may have operated on a shorter frequency than the Heinrich Stadials. We attribute these fluctuations to millennial-scale changes in the mean position of the westerlies.

Author contributions

BH conceived the project, which was initiated with the assistance of PB. BH and TL carried out the field work and collected the samples. BH analyzed the cosmogenic samples. BH and TL interpreted the data. PB provided regional oceanographic context. All authors contributed to the writing and editing of the paper.

Declaration of competing interest

The authors declare that they have no known competing financial interests or personal relationships that could have appeared to influence the work reported in this paper.

Acknowledgments

Funding for this project was provided by the National Geographic Society and by the University of Maine. Alexandra Balter and Jillian Pelto assisted in the field. We thank Mr. Antony Smith of Discovery Falklands, who was instrumental in providing logistical support, as well as staff at the South Atlantic Environmental Institute, who were key in providing critical contacts and information and for hosting us in Stanley. We also wish to thank staff in the Falkland Islands Government for assistance, Dr. Xavier Crosta for sea-ice data, Mrs. Gill Smith and the late Mr. Colin Smith, landowners, as well as Mr. Ken Morrison, Mr. Richard Fogerty, Mrs. Teresa Smith, and numerous others in the Falkland Islands who assisted us. Three reviewers provided useful comments that greatly improved this paper.

References

Anderson, R.F., Ali, S., Bradtmiller, L.I., Nielsen, S.H.H., Fleisher, M.Q., Anderson, B.E., Burckle, L.H., 2009. Wind-driven upwelling in the Southern Ocean and the deglacial rise in atmospheric CO_2. Science 323, 1443–1448.

Balco, G., Stone, J.O., Lifton, N.A., Dunai, T.J., 2008. A complete and easily accessible means of calculating surface exposure ages or erosion rates from (10)Be and (26)Al measurements. Quat. Geochronol. 3, 174–195.

Barker, S., Diz, P., 2014. Timing of the descent into the last Ice Age determined by the bipolar seesaw. Paleoceanography 29, 489–507.

Björck, S., Rundgren, M., Ljung, K., Unkel, I., Wallin, Å., 2012. Multi-proxy analyses of a peat bog on Isla de los Estados, easternmost Tierra del Fuego: a unique record of the variable Southern Hemisphere westerlies since the last deglaciation. Quat. Sci. Rev. 42, 1–14.

Broecker, W.S., 1998. Paleocean circulation during the last deglaciation: a bipolar seesaw? Paleoceanography 13, 119–121.

Broecker, W.S., Denton, G.H., 1989. The role of ocean-atmosphere reorganizations in glacial cycles. Geochem. Cosmochim. Acta 53, 2465–2501.

Buizert, C., Sigl, M., Severi, M., Markle, B.R., Wettstein, J.J., McConnell, J.R., Pedro, J.B., Sodemann, H., Goto-Azuma, -K., Kawamura, K., Fujita, S., Motoyama, H., Hirabayashi, M., Uemura, R., Stenni, B., Parrenin, F., He, F., Fudge, T.J., Steig, E.J., 2018. Abrupt ice-age shifts in southern westerly winds and Antarctic climate forced from the north. Nature 563, 681–685.

Caldenius, C.C., 1932. Las glaciaciones Cuaternarios en la Patagonia y Tierra del Fuego. Geogr. Ann. 14, 1–164.

Cheng, H., Edwards, R.L., Broecker, W.S., Denton, G.H., Kong, X., Wang, Y.-J., Zhang, R., Wang, X., 2009. Ice age terminations. Science 326, 248–252.

Clapperton, C.M., 1971. Evidence of cirque glaciation in the Falkland Islands. J. Glaciol. 10, 121–125.

Clapperton, C.M., Sugden, D.E., 1976. The maximum extent of glaciers in part of West Falkland. J. Glaciol. 17, 73–77.

Clark, R., 1972. Periglacial landforms and landscapes in the Falkland Islands. Biul. Peryglac. 21, 33–50.

Clark, P.U., Mix, A.C., 2002. Ice sheets and sea level of the last glacial maximum. Quat. Sci. Rev. 21, 1–7.

Clark, P.U., Dyke, A.S., Shakun, J.D., Carlson, A.E., Clark, J., Wohlfarth, B., Mitrovica, J.X., Hostetler, S.W., McCabe, A.M., 2009. The last glacial maximum. Science 325, 710–714.

Darvill, C.M., Bentley, M.J., Stokes, C.R., Shulmeister, J., 2016. The timing and cause of glacial advances in the southern mid-latitudes during the last glacial cycle based on a synthesis of exposure ages from Patagonia and New Zealand. Quat. Sci. Rev. 149, 200–214.

Darvill, C.M., Stokes, C.R., Bentley, M.J., Evans, D.J.A., Lovell, H., 2017. Dynamics of former ice lobes of the southernmost Patagonian Ice Sheet based on a glacial landsystems approach. J. Quat. Sci. 32, 857-856.

Davies, B.J., Darvill, C.M., Lovell, H., Bendle, J.M., Dowdeswell, J.A., Fabel, D., Garcia, J.L., Geiger, A., Glasser, N.F., Gheorgiu, D.M., Harrison, S., Hein, A.S., Kaplan, M.R., Martin, J.R.V., Mendelova, M., Palmer, A., Pelto, M., Rodés, A., Sagredo, E.A., Smedley, R., Smellie, J.L., Thorndycraft, V.R., 2020. The evolution of the Patagonian Ice Sheet from 35 ka to the present day (PATICE). Earth Sci. Rev. https://doi.org/10.1016/j.earscirev.2020.103152.

De Deckker, P., Arnold, L.J., van der Kaars, S., Bayon, G., Stuut, J.-B.W., Perner, K., Lopes de Santos, R., Uemura, R., Demuro, M., 2019. Marine Isotope Stage 4 in Australasia: a full glacial culminating 65,000 years ago: global connections and implications for human dispersal. Quat. Sci. Rev. 204, 187–207.

De Deckker, P., Moros, M., Perner, K., Jansen, E., 2012. Influence of the tropics and southern westerlies on glacial interhemispheric asymmetry. Nat. Geosci. 5, 266–269.

Denton, G.H., Hughes, T.J., 2002. Reconstructing the antarctic ice sheet at the last glacial maximum. Quat. Sci. Rev. 21, 193–202.

Denton, G.H., Anderson, R.F., Toggweiler, J.R., Edwards, R.L., Schaefer, J.M., Putnam, A.E., 2010. The last glacial termination. Science 328, 1652–1656.

Ditchburn, R.G., Whitehead, N.E., 1994. The Separation of ^{10}Be from Silicates. Third

Workshop of the South Pacific Environmental Radioactivity Association, pp. 4–7.
Doughty, A.M., Schaefer, J.M., Putnam, A.E., Denton, G.H., Kaplan, M.R., Barrell, D.J.A., Andersen, B.G., Kelley, S.E., Finkel, R.C., Schwartz, R., 2015. Mismatch of glacier extent and summer insolation in southern hemisphere mid-latitudes. Geology 43, 407–410.
Esper, O., Gersonde, R., 2014a. New tools for the reconstruction of Pleistocene Antarctic sea ice. Palaeogeogr. Palaeoclimatol. Palaeoecol. 399, 260–283.
Esper, O., Gersonde, R., 2014b. Quaternary surface water temperature estimations: new diatom transfer functions for the Southern Ocean. Palaeogeogr. Palaeoclimatol. Palaeoecol. 414, 1–19.
Fletcher, M.S., Moreno, P.I., 2012. Have the Southern Westerlies changed in a zonally symmetric manner over the last 14,000 years? A hemisphere-wide take on a controversial problem. Quat. Int. 253, 32–46.
Fogwill, C., Turney, C.S.M., Hutchinson, D., Taschetto, A., England, M., 2015. Obliquity control on Southern Hemisphere climate during the last glacial. Sci. Rep. 5, 11673. https://doi.org/10.1038/srep11673.
Garcia, J.L., Hein, A.S., Binnie, S.A., Gomez, G.A., Gonzalez, M.A., Dunai, T.J., 2018. The MIS 3 maximum of the Torres del Paine and Última Esperanza ice lobes in Patagonia and the pacing of southern mountain glaciation. Quat. Sci. Rev. 185, 9–26.
Hansom, J.D., Evans, D.J.A., Sanderson, D.C.W., Bingham, R.G., Bentley, M.J., 2008. Constraining the age and formation of stone runs in the Falkland Islands using optically stimulated luminescence. Geomorphology 94, 117–130.
Heusser, C., Heusser, L., Lowell, T., 1999. Palaeoecology of the southern Chilean lake district – isla grande de Chiloé during the middle-late llanquihue glaciation and deglaciation. Geogr. Ann. 81A, 231–284.
Jouzel, J., Masson-Delmotte, V., Cattani, O., Dreyfus, G., Falourd, S., Hoffmann, G., Minster, B., Nouet, J., Barnola, J.M., Chappellaz, J., Fischer, H., Gallet, J.C., Johnsen, S., Leuenberger, M., Loulergue, L., Luethi, D., Oerter, H., Parrenin, F., Raisbeck, G., Raynaud, D., Schilt, A., Schwander, J., Selmo, E., Souchez, R., Spahni, R., Stauffer, B., Steffensen, J.P., Stenni, B., Stocker, T.F., Tison, J.L., Werner, M., Wolff, E.W., 2007. Orbital and millennial antarctic climate variability over the past 800,000 years. Science 317, 793–797.
Kaplan, M.R., Strelin, J.A., Schaefer, J.M., Denton, G.H., Finkel, R.C., Schwartz, R., Putnam, A.E., Vandergoes, M.J., Goehring, B.M., Travis, S.G., 2011. In-situ cosmogenic ^{10}Be production rate at Lago Argentino, Patagonia: implications for late-glacial climate chronology. Earth Planet Sci. Lett. 309, 21–32.
Kaiser, J., Lamy, F., Hebbeln, D., 2005. A 70-kyr sea surface temperature record off southern Chile (Ocean Drilling Program Site 1233). Paleoceanography 20. https://doi.org/10.1029/2005PA001146.
Kelley, S.E., Kaplan, M.R., Schaefer, J.M., Andersen, B.G., Barrell, D.J.A., Putnam, A.E., Denton, G.H., Schwartz, R., Finkel, R.C., Doughty, A., 2014. High-precision ^{10}Be chronology of moraines in the Southern Alps indicates synchronous cooling in Antarctica and New Zealand 42,000 years ago. Earth Planet Sci. Lett. 405, 194–206.
Lal, D., 1991. Cosmic ray labeling of erosion surfaces: in situ nuclide production rates and erosion models. Earth Planet Sci. Lett. 104, 424–439.
Lister, D.H., Jones, P.D., 2015. Long-term temperature and precipitation records from the Falkland Islands. Int. J. Climatol. 35, 1224–1231.
Lisiecki, L.E., Raymo, M.E., 2005. A Plio-Pleistocene stack of 57 globally distributed benthic δ^{18}O records. Paleoceanography 20. https://doi.org/10.1029/2004PA001071.
Lorenz, E.N., 1968. Climatic determinism. Meterol. Monogr. 8, 1–3.
Lorenz, E.N., 1975. Climatic Predictability. GARP Publications Series, pp. 132–136.
Lorenz, E.N., 1976. Nondeterministic theories of climatic change. Quat. Res. 6, 495–506.
Mercer, J., 1984. Simultaneous climatic change in both hemispheres and similar bipolar interglacial warming: evidence and implications. Geophys. Monogr. 29, 307–313.
Milankovitch, M., 1941. Canon of Insolation and the Ice-Age Problem, vol. 132. Special Publications of the Royal Serbian Academy, p. 484.
Mix, A.C., Bard, E., Schneider, R., 2001. Environmental processes of the ice age: land, oceans, glaciers (EPILOG). Quat. Sci. Rev. 20, 627–657.
Murray, D.S., Carlson, A.E., Singer, B.S., Anslow, F.S., He, F., Caffee, M., Marcott, S.A., Liu, Z., Otto-Bliesner, B.L., 2012. Northern Hemisphere forcing of the last deglaciation in southern Patagonia. Geology 40, 631–634.
Nishiizumi, K., Imamura, M., Caffee, M.W., Southon, J.R., Finkel, R.C., McAninch, J., 2007. Absolute calibration of ^{10}Be AMS standards. Nucl. Instrum. Methods Phys. Res., Sect. B 258, 403–413.
Peterson, R.G., Whitworth III, T., 1989. The Subantarctic and Polar fronts in relation to deep water masses through the Southwestern Atlantic. J. Geophys. Res. 94, 10817–10838.
Putnam, A.E., Schaefer, J.M., Barrell, D.J.A., Vandergoes, M., Denton, G.H., Kaplan, M.R., Schwartz, R., Finkel, R.C., Goehring, B.M., Kelley, S.E., 2010. In situ cosmogenic ^{10}Be production-rate calibration from the Southern Alps, New Zealand. Quat. Geochronol. 5, 392–409.
Putnam, A.E., Schaefer, J.M., Denton, G.H., Barrell, D.J.A., Andersen, B.G., Koffman, T.N.B., Rowan, A.V., Finkel, R.C., Rood, D.H., Schwartz, R., Vandergoes, M.J., Plummer, M.A., Brocklehurst, S.H., Kelley, S.E., Ladig, K.L., 2013a. Warming and glacier recession in the rakaia valley, southern Alps of New Zealand, during Heinrich stadial 1. Earth Planet Sci. Lett. 382, 98–110.
Putnam, A.E., Schaefer, J.M., Denton, G.H., Barrell, D.J.A., Birkel, S.D., Andersen, B.G., Kaplan, M.R., Finkel, R.C., Schwartz, R., Doughty, A.M., 2013b. The last glacial maximum at 44°S documented by a ^{10}Be moraine chronology at Lake Ohau, southern Alps of New Zealand. Quat. Sci. Rev. 62, 114–141.
Roberts, D.E., 1984. Quaternary History of the Falkland Islands. Unpublished Ph.D. thesis, University of Aberdeen, Scotland.
Schaefer, J.M., Putnam, A.E., Denton, G.H., Kaplan, M.R., Birkel, S., Doughty, A.M., Kelley, S., Barrell, D.J.A., Finkel, R.C., Winckler, G., Anderson, R.F., Ninneman, U.S., Barker, S., Schwartz, R., Andersen, B.G., Schlüchter, C., 2015. The southern glacial maximum 65,000 years ago and its unfinished termination. Quat. Sci. Rev. 114, 52–60.
Shulmeister, J., Thackray, G.D., Rittenour, T.M., Hyatt, O.M., 2018. Multiple glacial advances in the Rangitata Valley, South Island, New Zealand, imply roles for Southern Hemisphere westerlies and summer insolation in MIS 3 glacial advances. Quat. Res. 89, 1–19.
Stone, J.O., 2000. Air pressure and cosmogenic isotope production. J. Geophys. Res. 105, 23753–23759.
Strand, P.D., Schaefer, J.M., Putnam, A.E., Denton, G.H., Barrell, D.J.A., Koffman, T.N.B., Schwartz, R., 2019. Millennial-scale pulsebeat of glaciation in the southern Alps of New Zealand. Quat. Sci. Rev. 220, 165–177.
Sugden, D.E., Clapperton, C.M., 1977. The maximum ice extent on island groups in the Scotia Sea, Antarctica. Quat. Res. 7, 268–282.
Toggweiler, J.R., Russell, J.L., Carson, S.R., 2006. Midlatitude westerlies, atmospheric CO_2 and climate change during the ice ages. Paleoceanography 21. https://doi.org/10.1029/2005PA001154.
Upton, J., Shaw, C.J., 2002. An overview of the oceanography and meteorology of the Falkland Islands. Aquat. Conserv. Mar. Freshw. Ecosyst. 12, 15–25.
WAIS Divide Project Members, 2013. Onset of deglacial warming in West Antarctica driven by local orbital forcing. Nature 500, 440–444.
WAIS Divide Project Members, 2015. Precise interpolar phasing of abrupt climate change during the last ice age. Nature 520, 661–665.
Wang, Y.J., Cheng, H., Edwards, R.L., An, Z.S., Wu, J.Y., Shen, C.-C., Dorale, J.A., 2001. A high-resolution absolute-dated late Pleistocene monsoon record from Hulu Cave, China. Science 294, 2345–2348.
Wang, Y.-J., Cheng, H., Edwards, R.L., Kong, X., Shao, X., Chen, S., Wu, J.Y., Jiang, X., Wang, X., An, Z.S., 2008. Millennial- and orbital-scale changes in the East Asian monsoon over the past 224,000 years. Nature 451, 1090–1093.
Wilson, P., Bentley, M.J., Schnabel, C., Clark, R., Xu, S., 2008. Stone run (block stream) formation in the Falkland Islands over several cold stages deduced from cosmogenic isotope (^{10}Be and ^{26}Al) surface exposure dating. J. Quat. Sci. 23, 461–473.
Zhu, J., Lücke, A., Wissel, H., Mayr, C., Enters, D., Ja Kim, D., Ohlendorf, C., Schäbitz, F., Zolitschka, B., 2014. Climate history of the Southern Hemisphere westerlies belt during the last glacial-interglacial transition revealed from lake water oxygen isotope reconstruction of Laguna Potrok Aike (52°S, Argentina). Clim. Past 10, 2153–2169.
Zolitschka, B., Anselmetti, F., Ariztegui, D., Corbella, H., Francus, P., Lücke, A., Maidana, N.I., Ohlendorf, C., Schäbitz, F., Wastegård, S., 2013. Environment and climate of the last 51,000 years – new insights from the Potrok Aike maar lake Sediment Archive Drilling prOject (PASADO). Quat. Sci. Rev. 71, 1–12.